1

2

3

4

5 **Transcriptome analysis of genetically matched human induced pluripotent**

6 **stem cells disomic or trisomic for chromosome 21.**

7

8 Patrick Gonzales*[†], Gin Fonte*[†], Christine Roberts*[†], Connor Jacobsen[†],

9 Gretchen H. Stein*[¶], Christopher D. Link*[†]

10

11

12 * Linda Crnic Institute for Down Syndrome, University of Colorado, Aurora, CO

13 80045

14

15 [†] Department of Integrative Physiology, University of Colorado, Boulder, CO

16 80309

17

18 [¶] Department of Molecular, Cellular, and Developmental Biology, University of

19 Colorado, Boulder, CO 80309

20

21   ***Transcriptome analysis in trisomy 21***

22

23   Key words:

24

25   RNA-seq, Down syndrome, cluster analysis, JunctionSeq, HERVH

26

27   Corresponding author:

28

29   Christopher D. Link, Ph.D.

30   Associate Professor

31   Linda Crnic Institute/Integrative Physiology

32   University of Colorado

33   Campus Box 354

34   Boulder, CO 80309

35

36   phone: 303 735-5112

37   email: linkc@colorado.edu

38   **Abstract**

39

40   Trisomy of chromosome 21, the genetic cause of Down syndrome, has the

41   potential to alter expression of genes on chromosome 21, as well as other

42   locations throughout the genome. These transcriptome changes are likely to

43   underlie the Down syndrome clinical phenotypes. We have employed RNA-seq

44   to undertake an in-depth analysis of transcriptome changes resulting from

45   trisomy of chromosome 21, using induced pluripotent stem cells (iPSCs) derived

46   from a single individual with Down syndrome. These cells were originally derived

47   by Li et al, who genetically targeted chromosome 21 in trisomic iPSCs, allowing

48   selection of disomic sibling iPSC clones. Analyses were conducted on

49   trisomic/disomic cell pairs maintained as iPSCs or differentiated into cortical

50   neuronal cultures. In addition to characterization of gene expression levels, we

51   have also investigated patterns of RNA adenosine-to-inosine editing, alternative

52   splicing, and repetitive element expression, aspects of the transcriptome that

53   have not been significantly characterized in the context of Down syndrome. We

54   identified significant changes in transcript accumulation associated with

55   chromosome 21 trisomy, as well as changes in alternative splicing and repetitive

56   element transcripts. Unexpectedly, the trisomic iPSCs we characterized

57   expressed higher levels of neuronal transcripts than control disomic iPSCs, and

58   readily differentiated into cortical neurons, in contrast to another reported study.

59   Comparison of our transcriptome data with similar studies of trisomic iPSCs

60   suggests that trisomy of chromosome 21 may not intrinsically limit neuronal

61   differentiation, but instead may interfere with the maintenance of pluripotency.

Gonzales et al. "Transcriptome analysis in trisomy 21"

62

63

64 **Introduction**

65

66   Down Syndrome (DS) results from an extra copy of chromosome 21, and this

67 change in gene dosage has been proposed to alter chromosome 21 gene

68 expression. Chromosome 21 trisomy also has the potential to alter the global

69 transcriptome, either by secondary effects of chromosome 21 gene over-

70 expression, or as a byproduct of additional genetic material itself. In addition to

71 the possible perturbation of specific cellular pathways by altered expression of

72 chromosome 21 genes, chromosome 21 also contains genes that impact the

73 global transcriptome directly. These include *ADARB1*, encoding one of two

74 genes responsible for adenosine-to-inosine RNA editing; U2AF1, a constitutive

75 splicing factor; and DYRK1A, a kinase known to target splicing factors.

76 Identifying transcriptome changes reproducibly caused by chromosome 21

77 trisomy may be crucial to understanding the origins of the clinical features of

78 Down Syndrome.

79

80   Initial gene expression studies that sought to establish chromosome 21-

81 dependent transcriptome changes using human material were confounded by the

82 effects of different genetic backgrounds in the DS and control individuals who

83 were studied (Gardiner et al, 2010). An alternative approach is to characterize

84 gene expression in inbred mouse DS models, which reproduce some of the

85 developmental and behavioral phenotypes of DS individuals (Liu et al, 2011).

4

86   Transcriptome studies have been done in multiple mouse DS models (Saran et

87   al, 2003; Potier et al, 2006; Ling et al, 2014; Guedj et al, 2015; Olmos-Serrano et

88   al, 2016), but no consistent pattern of transcriptome changes has been identified,

89   perhaps due to the different tissues and developmental stages analyzed in these

90   studies. In addition, these mouse DS models have triplication of chromosomal

91   regions syntenic to only part of human chromosome 21 as well as triplication of

92   non-chromosome 21 homologous genes, and thus may not capture the full

93   effects of human chromosome 21 trisomy.

94

95   Recently, the development of paired disomic/trisomic induced pluripotent stem

96   cells (iPSCs) derived from the same trisomic individual (or from discordant

97   monozygotic twins) has allowed the measurement of human trisomy 21-

98   dependent gene expression independent of genetic background differences (Li et

99   al, 2012: Weick et al, 2013; Jiang et al, 2013; LeTourneau et al, 2014). These

100   studies have consistently observed a general upregulation of genes on

101   chromosome 21, as well as highly variable significant gene expression

102   differences on other chromosomes. Li et al (2012) used an elegant genetic

103   selection system to derive disomic iPSC subclones from chr21 trisomic iPSCs

104   that were derived from an individual with Down syndrome. Based on an initial

105   microarray analysis, these researchers also reported a general upregulation of

106   chromosome 21 genes, but could identify only 3 non-chromosome 21 genes with

107   a > 2 fold dysregulation between disomic and trisomic iPSC pairs. We have used

108   RNA-seq to significantly extend this analysis using both disomic/trisomic iPSC

109   pairs and cortical neuron cultures derived from them. In addition to assaying

110   transcript accumulation, we have used the RNA-seq data to look for other

111   possible trisomy-induced transcriptome changes, including possible alterations in

112   adenosine-to-inosine RNA editing, alternative splicing, and repetitive element

113   expression.

114

115   In contrast to the Jiang et al study, the trisomic iPSCs we characterized were not

116   restricted in their ability differentiate into cortical neuron cultures, and in fact

117   showed higher expression of neuronal transcripts when compared to disomic

118   iPSCs. To investigate differences between our analyses and previous studies,

119   we have compared global gene expression data among the related studies, and

120   find evidence for at least two different states for trisomic iPSC. We suggest that

121   these different states may reflect an inherent inability for trisomic iPSCs to

122   maintain full pluripotency.

123

124   **Materials and Methods**

125

126   *iPSC Cell Culture*

127

128   Trisomic (C2 and C3) and disomic iPSC cell lines (C2-4-3, C2-4-4, C3-5-11,

129   and C3-5-13), which had been developed from an individual with Down

130   syndrome by Li et al. (2012), were obtained through the Linda Crnic Institute for

131   Down Syndrome (University of Colorado, Aurora, CO). These iPSC lines were

132   grown on Geltrex (Life Technologies) under feeder-free conditions in mTeSR1

133   medium according to the protocol of Stem Cell Technologies. iPSC colonies

134   were passaged with dispase, and differentiating colonies were removed manually

135   by scraping. Periodically, live iPSC colonies were stained with anti-Tra-1-60 or

136   Tra-1-81 conjugated to Dylight fluor 488 to confirm the stem cell character of the

137   colonies. Likewise, fixed cells were shown to express Oct4 by immunostaining.

138   We used ABI/Thermo Fisher TaqMan Copy Number Assays (Hs01180853_cn;

139   Hs02928366_cn; Hs01533676 corresponding to APP, DYRK1A and RCAN1

140   respectively) to evaluate the number of copies of Chr. 21 in the iPSC lines. We

141   found that C2 was stably trisomic, but that C3 appeared initially to be a mixture of

142   trisomic and disomic cells that rapidly gave rise to a consistently disomic cell line,

143   which we call C3-D21.

144

145   *Neuronal Differentiation*

146

147   iPSC cells were induced to differentiate to cortical neurons by a modification of

148   the method of Espuny-Camacho et al. (2013). Briefly, iPSCs were dissociated

149   with Accutase, and plated on Geltrex-coated dishes at 10-20 x 10^3 cells/cm^2 in

150   mTeSR1 medium + 10 uM Y27632 ROCK inhibitor (Tocris). After 2-4 days, the

151   cells formed a meshwork of dense ridges with mostly open spaces in between.

152   The differentiation process was begun (day 0) by feeding the cells every other

153   day for 12 days with NIM neural induction medium (Stem Cell Technologies),

154   followed by DDM medium supplemented with 2% B27 (Gaspard et al., 2009)

155   every other day for 12 days. On day 24, the dense ridges or islands containing

156   neural progenitors were manually dissociated, resuspended in DDM + 2% B27 +

157   10 uM Y27632, and plated on dishes and chamber slides coated with poly-

158   ornithine and laminin (Shi et al., 2012). Every 4-5 days, half the medium was

159   changed to fresh Neurobasal + 2% B27 + 2mM GlutaMax (Invitrogen). Colonies

160   that were clearly nonneuronal were removed by scraping, rinsing and refeeding

161   the cultures. After 40 days of differentiation, the cells were rinsed with PBS and

162   harvested with ice-cold Trizol or fixed with 4% para-formaldehyde + 4% sucrose

163   in PBS.

164

165   Successful differentiation of iPSCs into cortical neuronal cultures was confirmed

166   by immunofluorescence staining for markers of cortical layers V (transcription

167   factor Ctip2, encoded by BCL11B) and VI (transcription factor TBR1), as well as

168   for glutamatergic markers vGLUT1 (encoded by SLC17A7) and GRIK2 (see

169   Supplemental Figure 1).

170

171   *Immunofluorescence staining*

172

173   For live cell staining, StemGent antibodies conjugated to Dylight 488: Tra1-60

174   or Tra1-81, were applied to iPSC cultures for 30-60 min according the

175   manufacturer's instructions, and the stained colonies were examined with an

176   Evos FL microscope.

177

178   For staining of fixed cells, cells were grown on chamber slides (LabTek II CC2),

179   rinsed with Dulbecco's PBS, fixed 15 min in 4% p-formaldehyde/4% sucrose in

180   PBS, permeabilized 7 min in 0.25% Triton X-100 in PBS, and blocked 1-2 hrs

181   with 5% sheep or goat serum in PBS. Primary antibodies, applied overnight at

8

182   4°C, were from Abcam: Oct4 (ab19857), Tbr1 (ab31940), Ctip2 (ab18465),

183   GRIK2 (ab53092), vGlut1 (ab72311) and βIII-tubulin (ab7751); from Millipore:

184   MAP2 (polyclonal AB5622), MAP2 (monoclonal MAB3418). The slides were

185   rinsed (5X PBS), secondary antibodies (Life Technologies) were applied for 2 hrs

186   at room temperature, rinsed (4X PBS), stained with DAPI (Sigma D9542), and

187   mounted with ProLong Gold AntiFade (Life Technologies). Images were

188   captured using an epifluorescence microscope (Zeiss Axioskop) equipped with a

189   CCD camera and Slidebook image analysis software (3i).

190

191   *Immunoblotting*

192

193   Lysates of disomic and trisomic iPSCs were prepared with RIPA buffer

194   containing protease and phosphatase inhibitor cocktails (Sigma), and the protein

195   content of each lysate was determined (Bradford assay). Using BioRad reagents

196   and equipment, an equal amount of protein from each lysate was denatured by

197   boiling 5 minutes in 4x Sample Buffer containing DTT; run on a Criterion XT pre-

198   cast gradient gel (4%-12%) in XT-MOPS running buffer at 150 volts for 1.5-2

199   hours; and blotted via a Trans-Blot Turbo system for 7 minutes using the Mixed

200   Molecular Weight protocol (2.5A, up to 25V). The blot was washed in TBS-T,

201   (tris-buffered saline containing Tween 20), stained with Ponceau S to affirm

202   protein transfer, washed again and blocked in 5% milk in TBS-T before being

203   stained sequentially with MAP2 rabbit polyclonal antibody (1:1000, Abcam

204   ab32454) and goat anti-rabbit HRP (1:1000). The washed blot was then treated

205   with SuperSignal West Femto Maximum Sensitivity substrate (Life

206   Technologies), diluted 1:10 in distilled water, for 5 minutes while covered, and

207   images were taken using a ChemiDoc-it imaging system and VisionWorks LS

208   software. The blot was stripped and stained for GAPDH (1:2000) as a loading

209   control. Images were analyzed using Fiji (ImageJ) and Excel; integrated density

210   of each band was measured and normalized to the GAPDH signal before

211   comparing the amount of MAP2 in each protein sample.

212

213   *RNA isolation, cDNA library preparation, high throughput sequencing*

214

215   RNA for poly(A) RNA sequencing libraries was extracted from IPSC and

216   neuronal cultures via TRIzol extraction. Genomic DNA was removed using

217   TURBO DNase (Invitrogen). RNA integrity (RIN) was verified on an Agilent 2100

218   bioanalyzer and only samples with RIN ≥ 7.0 were used for sequencing. Single-

219   end sequencing libraries were prepared by the UCCC Genomics Core (Aurora,

220   CO) using the TruSeq Stranded mRNA Library Prep Kit (Illumina). Cluster

221   generation and sequencing were performed on the Illumina HiSeq 2000 platform.

222   The reads were de-multiplexed and converted to FASTQ format using CASAVA

223   software from Illumina.

224

225   *Analysis of RNA-seq data*

226

227   Analysis of library complexity and per-base sequence quality (i.e. q > 30) was

228   assessed using FastQC (v0.11.2) software (Andrews, 2010). Low quality bases

229   (q < 10) were trimmed from the 3' end of reads. Adaptor sequences and reads

230   shorter than 40 nucleotides were removed using Trimmomatic (Bolger, 2014).

231   Reads were aligned to GRCh37/hg19 using TopHat2 (v2.0.14, --b2-very-

232   sensitive --keep- --no-coverage-search --library-type fr-firststrand) (Kim et al.,

233   2013). High quality mapped reads (MAPQ > 10) were filtered with SAMtools

234   (v0.1.19) (Li et al., 2009). Gene level counts were obtained using the GRCh37

235   Ensembl annotation with Rsubread (v 1.18.0, strandSpecific = 2,

236   GTF.featureType = "exon", countMultiMappingReads = FALSE) (Liao, 2013).

237   Differential expression of genes was determined using DESeq (v1.24.0) software

238   with the options "per-condition", "maximum", and "local" for dispersion

239   calculations (Anders, 2010). Significance was assigned to genes with an FDR

240   less than 10%.

241

242   *Global RNA Editing*

243

244   The bioinformatics scheme was implemented to specifically quantify the amount

245   of RNA editing that occurs in known RNA editing locations. With this is mind we

246   used the "DAtabase of RNa Editing" (DARNED) to procure a list of all previously

247   published RNA editing locations in the human genome (hg19) (Kiran, 2010). Only

248   Adenosine to Inosine RNA editing sites in exons were used in the analysis.

249   Reads overlapping DARNED locations were kept if they were uniquely aligned

250   with a MAPQ greater than 10, and a minimum PHRED score of 30 at the

251   nucleotide level. An edit ratio was then determined for each location by summing

252   the total number of edits (A to G changes) divided by the total possible edits

253   (read depth at edit location). A minimum read depth of 10 was required for the

11

254   edit ratio to be determined. The global editing percentage for each sample was

255   then ascertained by averaging all edit ratios considered.

256

257   *Alternative splicing analysis*

258

259   Splicing analysis was performed using Hartley's QoRTs / JunctionSeq pipeline

260   (Hartley, 2016). Tophat aligned reads and an Ensembl annotation file (GRCh37)

261   were used as input to generate gene counts with QoRTs software using the

262   options "--stranded", "--singleEnded", and "--minMAPQ 50". A flat annotation file

263   containing known splice junctions was produced in QoRTs using the same

264   Ensembl annotation above with the "--stranded" option set. The QoRTs

265   generated files were both used as input into JunctionSeq for differential exon and

266   splice junction analysis. Exons or splice junctions were considered differentially

267   expressed in the disomic vs. trisomic comparison if the adjusted P value was less

268   than 10%.

269

270   *Semi-quantitative PCR*

271

272   To capture the exclusion of APOO exon 4 in trisomic samples we designed

273   primers bordering exon 3 and 5 (FWD 5' TCTCACAGCTCCGACACTAT 3', REV

274   5' GAGTCCAATAAGGCCAGCAA 3'). 30ng/ul of cDNA were used as input for

275   all samples. PCR cycling conditions were set as follows: denaturation for 5 min at

276   95 °C, followed by 40 cycles of denaturation for 30 s at 94 °C, annealing for 30 s

277   at 54 °C, and polymerization for 30s at 72 °C, and a final extension for 10 min at

278   72 °C. APOO exon 4 exclusion was resolved on 2% agarose gel.

279

280   *Expression of repetitive elements*

281

282   RepEnrich software was used to generate a count table containing uniquely

283   aligned reads assigned to repetitive elements (Criscione et al., 2014). An hg19

284   repeatmasker file was used to build the repetitive element annotation. Size

285   factors generated from the DESeq gene expression analysis were used to

286   normalize the samples. DESeq (v1.24.0) was used to determine differential

287   expression of repetitive element transcripts. Significance was assigned to genes

288   with an FDR less than 10%.

289

290   *Cluster analysis of datasets.*

291

292   The full datasets of normalized transcript accumulation values for the iPSC

293   studies by Weick et al, 2013; Jiang et al, 2013; and LeTourneau et al, 2014 were

294   downloaded from the Gene Expression Omnibus (GSE48611, GSE47014, and

295   GSE55504, respectively). Trisomic/disomic ratios were calculated using the

296   averaged transcript levels for all genes assayed in each study. Ratios were

297   imported into Cluster 3.0 (de Hoon et al, 2004) for genes identified as

298   significantly differentially expressed in our study, and present in 6/7 of the studies

299   being compared. The ratios were log-transformed, and hierarchical clustering

300   was performed using centroid linkage and centered correlation for the similarity

301   matrix. The clustering output was visualized using Java TreeView (Saldanha,

302   2004).

303

304

305

306

307

308   **Results**

309

310   *Generation of RNA-seq data*.

311

312   Paired trisomic/disomic iPSCs were obtained from the Russell lab and

313   maintained in feeder-free media. Cortical neuronal cultures were derived from

314   the iPSCs following the procedure of Espuny-Camacho et al (2013) with minor

315   modifications (see Materials and Methods) and harvested after 40 days in

316   culture. All sequence data was generated from polyA-selected, strand-specific

317   sequencing libraries by Illumina sequencing (100-115 bp single end reads). The

318   iPSC data was generated from 3 independent preps of trisomic clone C2 from

319   the Russell lab, and 3 independent preps of disomic sub-clones derived from the

320   C2 lineage (two C2-4-4 and one C2-4-3). Our analysis of the transcriptomes of

321   cortical neurons compared 3 biologically independent sets of differentiated

322   cortical neurons derived from the trisomic C2 line and from disomic C3 iPSC cells

323   (C3-D21, which arose spontaneously from trisomic clone C3). Differentially

324   expressed transcripts were identified using the DESeq algorithm. Principal

14

325   component analysis demonstrated that the 12 transcriptome datasets partitioned

326   as expected (see Figure 1).

327
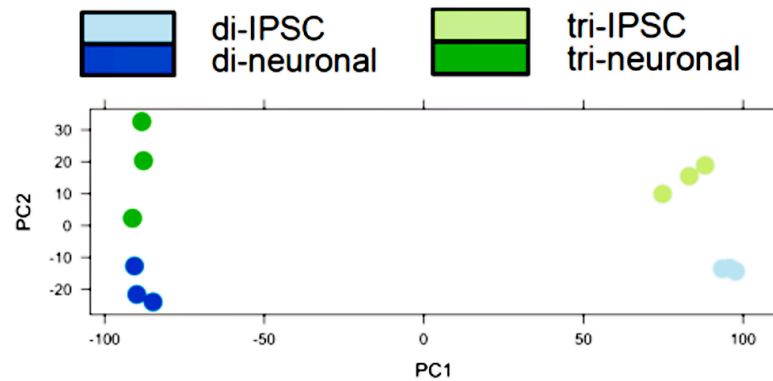
328

Figure 1. Principal component analysis of transcriptome datasets. Note principal component 1 clearly segregates iPSC from neuronal cultures, while component 2 partitions trisomic from disomic cells.

329

330   *Gene expression in trisomic cells.*

331

332   Using a false discovery rate (FDR) of 10%, we identified 1644 transcripts (810

333   up, 834 down) with differential expression between trisomic and disomic iPSCs

334   (see Supplementary table 1). Gene ontology analysis revealed that trisomic

335   iPSCs had increased transcript levels for genes involved in neurogenesis and

336   neuronal function (see Table 1). In contrast, genes with decreased transcripts in

337   the trisomic iPSCs were heavily over-represented in cell adhesion function and

338   germ layer/mesoderm development. The germ layer category includes genes

339   well-established to function in maintenance of stem cell fates (e.g., KLF4,

340   NODAL, LEFTY1 and 2, etc).

341

15

Up in trisomic iPSCs

Functional cluster #1	Fold Enrichment	PValue	FDR
transmission of nerve impulse	3.96	8.90E-16	1.54E-12
synaptic transmission	3.88	6.27E-13	1.09E-09
cell-cell signaling	2.84	8.56E-13	1.49E-09
neurological system process	1.74	2.92E-06	0.00509259
Functinal cluster #2			
regulation of system process	3.37	5.80E-10	1.01E-06
regulation o ftransmission of nerve impulse	4.52	6.31E-09	1.10E-05
regulation of neurological system process	4.35	1.35E-08	2.34E-05
regulation of synaptic transmission	4.46	4.20E-08	7.32E-05
regulation of synaptic plasticity	3.61	0.00635158	10.5118869
Functinal cluster #3			
neuron differentiation	3.17	3.89E-12	6.77E-09
neuron development	3.15	1.93E-09	3.37E-06
cell morphogenesis involved in differentiation	3.55	6.04E-09	1.05E-05
cell morphogenesis involved in neuron differentiation	3.60	6.05E-08	1.06E-04
cell morphogenesis	2.84	7.80E-08	1.36E-04
neuron projection morphogenesis	3.53	8.80E-08	1.53E-04
cell projection morphogenesis	3.30	9.94E-08	1.73E-04
cell part morphogenesis	3.16	2.47E-07	4.31E-04
neuron projection development	3.16	2.47E-07	4.31E-04
axonogenesis	3.44	8.72E-07	0.00152002
cellular component morphogenesis	2.55	1.02E-06	0.0017711
cell projection organization	2.51	4.34E-06	0.00756051
axon guidance	3.51	3.15E-04	0.54781196
cell motion	1.95	5.13E-04	0.89116623

Down in trisomic iPSCs

Functional cluster #1	Fold Enrichment	P Value	FDR
cell adhesion	2.75	2.03E-12	3.55E-09
biological adhesion	2.74	2.12E-12	3.71E-09
homophilic celladhesion	5.38	6.15E-10	1.08E-06
cell-cell adhesion	3.14	5.10E-07	8.92E-04
Functional cluster #2			
gastrulation	6.87	2.54E-08	4.44E-05
formation of primary germ layer	8.82	2.81E-07	4.92E-04
embryonic morphogenesis	3.03	3.60E-07	6.29E-04
pattern specification process	3.12	9.48E-07	0.00165705
mesoderm morphogenesis	8.44	1.84E-06	0.00321333
mesoderm development	5.63	2.70E-06	0.0047194
mesoderm formation	8.01	1.16E-05	0.02024587
anterior/posterior pattern formation	3.66	3.04E-05	0.05307399
regionalization	3.09	4.39E-05	0.07681769
tissue morphogenesis	3.03	1.60E-04	0.27891177
tube morphogenesis	3.03	0.00203497	3.49910234
embryonic development ending in birth or egg l	1.92	0.0085742	13.9779643
chordate embryonic development	1.84	0.01582799	24.3434896
Functional cluster #3			
smooth muscle contraction	8.74	5.77E-06	0.01008282
muscle contraction	3.14	3.01E-04	0.52510993
muscle system process	2.86	7.74E-04	1.3448919

Up in trisomic neuronal culture

Functional cluster #1	Fold Enrichment	PValue	FDR
gamma-aminobutyric acid signaling pathway	29.41	3.09E-04	0.48116101
neurological system process	1.94	0.01463154	20.5505489
synaptic transmission	3.45	0.01518596	21.245381
transmission of nerve impulse	2.94	0.03052941	38.3633337
cell-cell signaling	2.21	0.04863405	54.0738732
Functional cluster #2			
cell adhesion	2.31	0.01895984	25.8260635
biological adhesion	2.31	0.01912934	26.0258249
cell-cell adhesion	2.66	0.11533904	85.2320977
Functional cluster #3			
mechanical stimulus involved in sensory perception	33.93	0.00332655	5.06765519
detection of mechanical stimulus	27.57	0.00505111	7.59925072

Down in trisomic neuronal culture

Functional cluster #1	Fold Enrichment	PValue	FDR
cell adhesion	2.56	6.45E-18	1.17E-14
biological adhesion	2.56	7.10E-18	1.29E-14
cell-cell adhesion	2.34	5.88E-06	0.01065966
Functional cluster #2			
blood vessel development	3.24	2.11E-11	3.82E-08
vasculature development	3.17	4.71E-11	8.53E-08
angiogenesis	4.00	5.25E-11	9.52E-08
blood vessel morphogenesis	3.24	6.71E-10	1.22E-06
Functional cluster #3			
extracellular matrix organization	4.44	1.01E-09	1.82E-06
collagen fibril organization	7.65	1.50E-07	2.72E-04
extracellular structure organization	3.06	6.24E-07	0.00113042

342

343 **Table 1.** Gene ontology enrichment using DAVID (*https://david.ncifcrf.gov/*).

344

345   To confirm the surprising observation that the trisomic iPSCs appeared to

346 express neuronal transcripts at higher levels than the paired disomic iPSCs, we

347 focused on MAP2, a classic neuronal-specific microtubule-binding protein whose

348 transcript was increased an average of 6 fold in the trisomic iPSCs compared to

349 the disomic iPSCs. As shown in Figure 2, MAP2 protein was also significantly

350 increased in the trisomic iPSCs as assayed by either immunoblot or
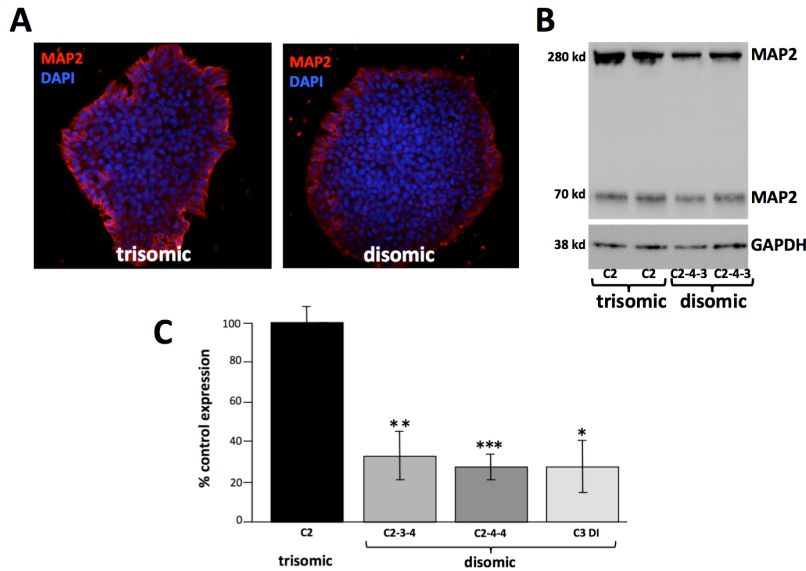
351 immunofluorescence.

Figure 2. Trisomic iPSCs show higher levels of MAP2 expression. A. iPSC colonies fixed and stained for MAP2. **B.** Representative immunoblot from trisomic and disomic iPSCs. Note two MAP2 isoforms are detected. **C.** Quantitation of MAP2 immunoblots. (* = P<0.02, ** = P< 0.01, ***, P< 0.001, paired T-tests)

352

353

354   Letourneau et al (2014) claimed to identify gene expression dysregulation

355   domains (GEDDs) in trisomic iPSCs and fibroblasts.   We applied the same

356   algorithmic approach to our iPSC data, and either did not see the same patterns

357   of expression domains (see Supplemental Figure 2) or did not detect statistically

358   significant expression domains.

359

360   Using the same parameters applied in the iPSC comparison to the RNA-seq

361   data from the neuronal cultures, we identified 1,377 transcripts (212 up in

362   trisomic cells, 1165 down) differentially expressed in the trisomic and disomic

363   neuronal cultures (See Supplementary Table 2). Gene ontology analysis of

364   differentially expressed transcripts (Table 1) identified similar functional

365   categories as observed in the precursor iPSCs. Transcripts for many GABA and

366   glutamate receptors were markedly increased in the trisomic neuronal cultures.

367   We note that transcripts for general neuronal markers (e.g., MAP2, βIII tubulin,

368   and SNAP25) were not increased in the trisomic neuronal cultures compared to

17

369   the disomic neuronal cultures, suggesting that the increases in synaptic markers

370   in the trisomic neuronal cultures were not simply the result of a greater proportion

371   of neurons in these cultures, but rather reflect functional differences in the

372   neurons themselves. This observation seems to differ from the results of Weick

373   et al (2013), who observed reduced synaptic activity in their trisomic iPSC-

374   derived neuronal cultures. As observed for the iPSCs, many categories of cell

375   adhesion molecules showed decreased transcript accumulation in the trisomic

376   neuronal cultures. (One class of cell adhesion-associated transcripts was

377   increased in the trisomic neuronal cultures, however, this class encodes

378   predominantly neuronal-specific adhesion molecules such as *DAB1*, *CDH18*, and

379   *NELL2*.) As expected, stem cell-associated transcripts were expressed at low

380   levels in both the trisomic and disomic neuronal cultures, with no significant

381   differential expression.

382

383   In both the iPSC and neuronal trisomic cultures, chromosome 21 transcripts

384   were increased overall, at close to the 1.5 fold increase predicted from a simple

385   gene dosage effect, however, the specific chromosome 21 genes over-

386   expressed was dependent on the cell types being analyzed (Figure 3)
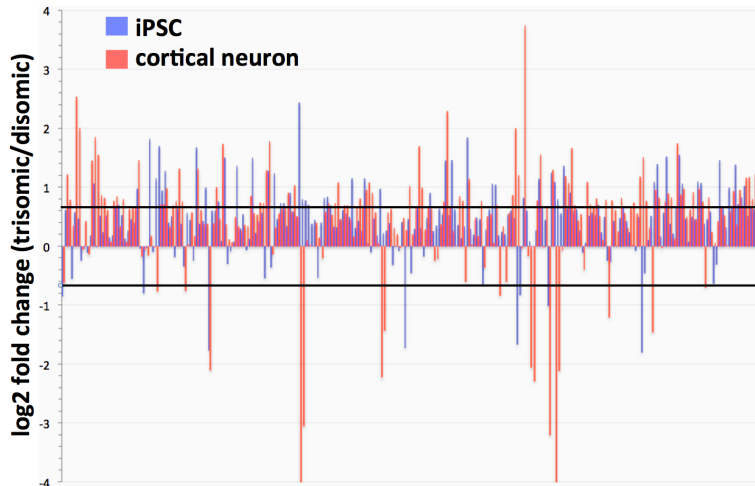
Figure 3. Expression of Chr 21 genes in iPSCs and cortical neuronal cultures (trisomic/disomic ratios). Lines represent individual gene ratios across chromosome 21. Note strong general trend for Chr 21 genes to be over-expressed, although specific genes may be strongly up- or-down regulated depending on cell type. (Black lines indicate 1.5 fold increases or decreases in trisomic cells.)

387

388   *Adenosine-to-inosine (A-to-I) editing in trisomic cells.*

389

390   ADARB1 encodes one of the two enzymes responsible for post-transcriptional

391   A-to-I editing of RNA. This gene is encoded on chromosome 21, leading to

392   suggestions that excessive RNA editing may occur in trisomy 21 cells. To test

393   this hypothesis, we scored editing levels at ~10,000 residues annotated to

394   undergo A-to-I editing (the DARNED database) in the trisomic and disomic

395   neuronal cultures. (We did not score editing in the iPSCs, as A-to-I editing

396   happens preferentially in neuronal cells, and in fact the iPSCs had very low levels

397   of ADARB1 transcripts.) We found that ADARB1 transcripts are increased in the

398   trisomic neuronal cultures, however levels of these transcripts do not correlate

399   well with over all levels of A-to-I editing (see Figure 4). We conclude that

400   increased levels of ADARB1 transcripts do not lead to increases in global RNA

401   editing. Our dataset does not have sufficient read depth to determine rigorously

402   if there were significant changes in site-specific editing in the trisomic neuronal
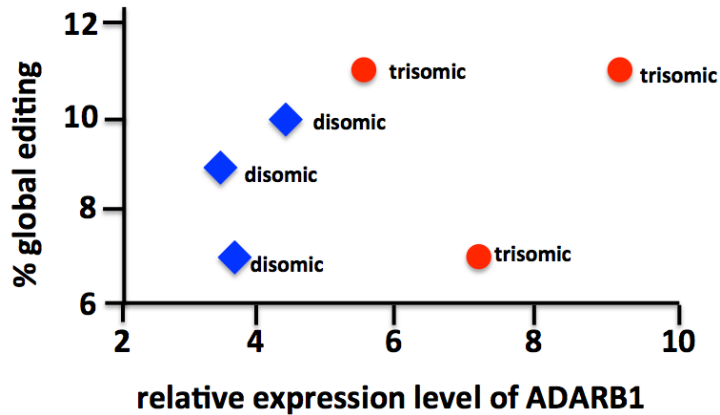
403   cultures.

Figure 4. Correlation between ADARB1 transcript abundance and levels of global A-to-I editing. Note that all trisomic cultures had higher normalized levels of ADARB1 transcripts, but this did not necessarily translate into higher editing rates.

404

405   *Splicing alterations in trisomic cells.*

406

407   To identify differences in splicing between trisomic and disomic cells, we tested

408   multiple splicing algorithms, and chose JunctionSeq (see Methods). Using this

409   algorithm we identified 117 annotated genes with splicing changes when

410   comparing trisomic and disomic iPSCs, and 36 such genes when comparing the

411   derived cortical neuron cultures (using a conservative adjusted P value < 0.01).

412   (See Supplemental Table 3.) Only one gene, SLC38A2, appeared to have

413   altered splicing in both the iPSCs and cortical neuronal cultures, perhaps not

414   surprising given the large transcriptional and splicing differences between stem

415   cells and neurons. To verify this bioinformatic analysis, we performed semi-

416   quantitative RT-PCR on a subset of genes identified in the iPSC analysis.

417   Shown in Figure 5 are the results for the Apolipoprotein O gene (APOO). As

418   predicted by the JunctionSeq analysis, trisomic cells show increased exclusion of
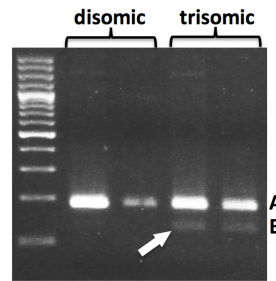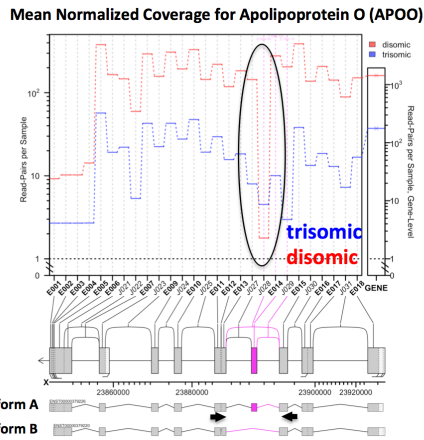
419   exon 14.

420

Figure 5. Altered splicing pattern of APOO in trisomic cells.
A. JunctionSeq output supporting the skipping of exon 14 in trisomic iPSCs.
B. RT-PCR targeting exon 14 exclusion (primer locations shown by arrows in panel A). Arrow indicates exon exclusion band only recovered in trisomic cells.

421

422

423   *Accumulation of repetitive element transcripts in trisomic cells.*

424

425   Retrotransposons, one class of repetitive elements, appear to play an important

426   role in the maintenance of stem cell pluripotency (Macfarlan et al, 2012; Fort et

427   al, 2014). To determine whether chromosome 21 trisomy might impact the

428   accumulation of repetitive element (RE) transcripts globally, we used the

429   RepEnrich algorithm (Criscione et al, 2014) to compare RE transcript levels in

430   both the iPSC and differentiated neuronal trisomic/disomic culture pairs (see

431   Supplemental table 4). In the iPSC comparison, there was a trend towards

432   decreased RE transcript accumulation in the trisomic cells, with 26/38

433   differentially expressed RE transcripts (FDR <10%) lower in the trisomic cells.

434   Interestingly, the most highly expressed RE transcript in the iPSCs was HERVH-

435   int, which also showed the most (statistically) significant difference between the

436   trisomic and disomic iPSCs: a > 3 fold reduction in the trisomic cells. There was

437   no significant difference in HERVH-int expression in cortical neuronal cultures,

438   and the overall trend in RE expression appeared reversed, with 18/21

439   significantly different RE transcripts increased in the trisomic cells.

21

440

441   *Comparison to other transcriptome data sets.*

442

443   The iPSCs and induced neuronal cultures that we have characterized were

444   derived from a single individual, thereby intrinsically limiting the generalization of

445   our results. However, three datasets have been published that have attempted a

446   similar transcriptome characterization using trisomic/disomic iPSC pairs that

447   have the same genetic background within each study (Table 2). Weick et al

448   (2013) derived iPSCs from fibroblasts from a DS individual who was mosaic for

449   chromosome 21 trisomy, which allowed the derivation of both trisomic and

450   disomic iPSCs. Jiang et al (2013) used an elegant, inducible XIST-based system

451   to inhibit expression of one chromosome 21 in trisomic iPSC clones, which also

452   allowed a trisomic/disomic comparison in the same iPSC clone. Letourneau et al

453   (2014) identified a rare set of monozygotic twins discordant for chromosome 21

454   trisomy, and that enabled them to derive a trisomic/disomic iPSC pair. As we

455   have done, these studies all used statistical criteria to generate lists of genes

456   with differential expression in trisomic vs. disomic iPSCs. Comparison of these

457   lists identified no differentially expressed gene common to all the studies, except

458   for genes expressed on chromosome 21. There are multiple, non-mutually

459   exclusive, possible explanations for this observation: inherent variability in

460   independently-generated iPSCs, large effects of the experimental conditions

461   used in individual labs, insufficient replication to identify all transcriptome

462   differences accurately, strong effects of genetic background, one or more study

463   with outlying data, or a fundamental absence of a non-chromosome 21

22

464   transcriptome signature in trisomic iPSCs. To sort through these possibilities, we

465   undertook a cluster analysis to determine how the datasets grouped. In

466   particular, we sought to determine if our dataset was truly an outlier in

467   comparison to the previous studies.

study	isogenic iPSC approach	sex	transforming factors	culture	transcriptome analysis
Li et al, 2012 (used in our study)	genetic selection for Chr 21 loss	M	LIN28, NANOG, SOX2, OCT4	feeder-free	RNA-seq
Weick et al, 2013	fibroblasts from mosaic individual	M	OCT4, SOX2, KLF4, MYC	MEFs	microarray
Jiang et al, 2013	inducible XIST inactivation of one Chr 21	M	OCT4, SOX2, KLF4, MYC	MEFs	microarray
Letourneau et al, 2014	fibroblasts from discordant twin pair	F	OCT4, SOX2, KLF4, MYC	human foreskin	RNA-seq

468

469   **Table 2. Comparable studies assaying transcriptome differences in isogenic**

470   **disomic/trisomic iPSCs pairs.**

471

472   The relevant data from previous studies were downloaded from online

473   repositories, and trisomic/disomic ratios were calculated for all the annotated

474   genes assayed. This approach enabled us to use a dimensionless measure that

475   allowed comparison of RNA-seq and microarray data. Our study and the twin

476   study by Letourneau et al (2014) produced single sets of trisomic/disomic ratios.

477   The study by Weick et al (2013) generated two sets of ratios, using the data from

478   two trisomic clones (DS1 and DS4) and one disomic clone (DS2). (We

479   calculated the DS1/DS2 and DS4/DS2 ratios to maximize information, while

480   appreciating that these ratios are not independent because they use the same

481   denominator.) The study by Jiang et al (2013) examined 3 independent XIST

482   chromosome 21 insertion subclones derived from the same parental trisomic

483   iPSC clone. These subclones were subjected to doxycyline-induced XIST
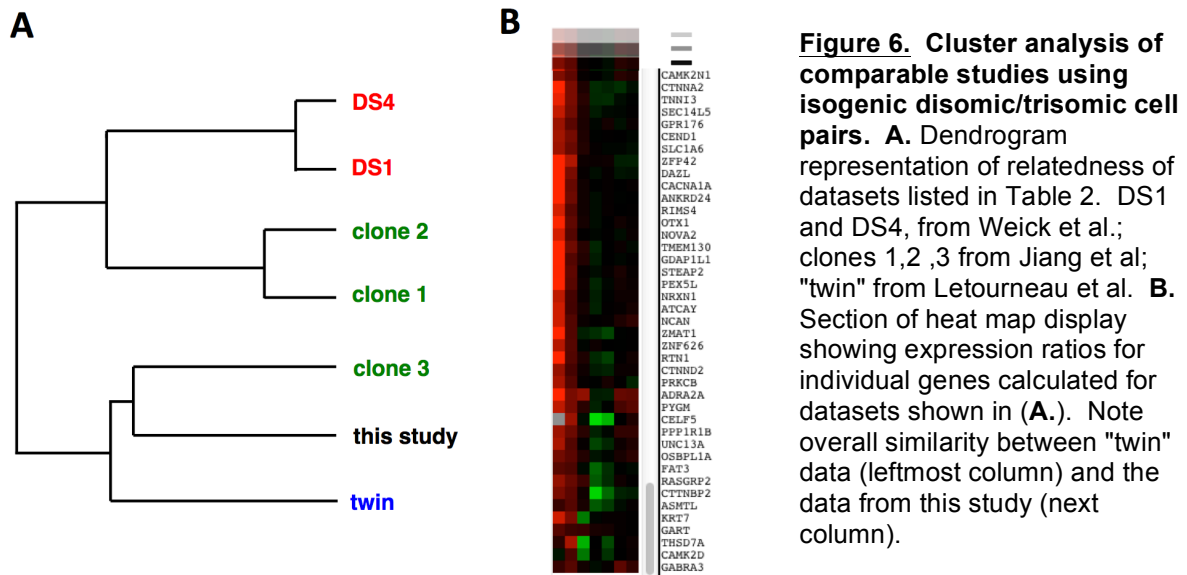
484   silencing, and trisomic/disomic ratios could be calculated by comparing

485   uninduced/induced transcriptome measurements, thus generating 3 independent

486   ratios (clones 1, 2, 3). The cluster analysis was based on the trisomic/disomic

487   ratios of our set of differentially expressed genes and the calculated ratios for the

488   same genes in the other datasets. After filtering for genes with values in at least

489   5/6 of the other datasets, 942 genes were used for the clustering analysis (see

490   Materials and Methods).

491

492   Figure 6A shows the dendrogram of the calculated dataset relationships. Note

493   that our dataset does not appear to be an outlier, but instead clusters with clone

494   3 of the study by Jiang et al (2013) and with the twin study of Letourneau et al.

495   (2014). Figure 6B shows a portion of the gene expression heat map for the

496   clustered datasets, capturing genes that had increased expression (red color) in

497   our dataset (second column in heat map display). Note that these genes include

498   neuron-associated transcripts such as neurexin (NRXN1), neurocan (NCAN),

499   and α-2A adrenoreceptor (ADRA2A), all of which also show increased

500   expression in the trisomic iPSCs characterized in the twin study of Letourneau et

501   al (2014; first column in heat map display).

A

B

Figure 6. Cluster analysis of comparable studies using isogenic disomic/trisomic cell pairs. A. Dendrogram representation of relatedness of datasets listed in Table 2. DS1 and DS4, from Weick et al.; clones 1,2 ,3 from Jiang et al; "twin" from Letourneau et al. **B.** Section of heat map display showing expression ratios for individual genes calculated for datasets shown in (**A.**). Note overall similarity between "twin" data (leftmost column) and the data from this study (next column).

502

503   **Discussion.**

504

505   *Transcript accumulation differences between cells trisomic or disomic for*

506   *chromosome 21.*

507

508   An inherent limitation of human transcriptome studies is accounting for the

509   differing genetic background of individuals. In the context of Down syndrome,

510   this limitation has hindered determining the degree to which trisomy of

511   chromosome 21 alters expression of genes on this chromosome and in the

512   genome as a whole. However, recent technical advances have allowed the

513   derivation of iPSCs trisomic or disomic for chromosome 21 from the same

514   individual. We have used RNA-seq to characterize in depth the transcriptome of

515   one such trisomic/disomic iPSC pair, originally generated by Li and colleagues

516   (Li et al, 2012). We have also differentiated these iPSCs into cortical neuronal

517   cultures to investigate how trisomy of chromosome 21 impacts the transcriptome

518   in differentiated neurons. Our results indicate that an increase in chromosome

519   21 dosage does generally lead to increased transcript accumulation for

520   chromosome 21 genes. However, not all chromosome 21 genes follow this

521   pattern, and which genes show increased expression depends on the cell type

522   assayed (iPSCs vs. differentiated cortical neurons). This observation may not be

523   surprising, given how regulatory loops, compensatory changes, and cell-specific

524   transcriptional programs may modulate or override the dosage effect on any

525   given chromosome 21 gene. In this regard, it has recently been reported

526   (Sullivan et al, 2016) that the interferon response is up-regulated in trisomy 21

527   fibroblasts and lymphoblast lines, likely due to increased expression in these

528   cells of the four interferon receptors (IFNAR1, IFNAR2, IFNGR2, and IL10RB)

529   located on chromosome 21. We find that these receptors also have increased

530   transcript accumulation in the trisomic iPSCs we analyzed, but this is not

531   apparent in the derived neuronal cultures.

532

533   As observed in other studies, the majority of significant transcriptome changes

534   we identified in both iPSCs and derived neuronal cultures occur in non-

535   chromosome 21 genes. Gene ontology analysis of genes with transcript

536   abundance changes in trisomic iPSCs unexpectedly revealed increases in

537   transcripts from neuronal-associated genes and decreases in transcripts from

538   genes involved in cell adhesion function and germ layer/mesoderm development.

539   These differences did not result from visible spontaneous differentiation in the

540   trisomic iPSCs, which were monitored daily. We note, however, that cells in

541   iPSC cultures are not homogeneous (see Figure 2), and one interpretation of our

542   results is that the trisomic iPSC cultures contain higher proportions of stem cells

543   biased towards neuronal development.

544

545   One significant consideration in comparing the trisomic and disomic iPSCs used

546   in this study is that the disomic clones have gone through two cycles of selection:

547   first with G418 to select for the insertion of a dual selection cassette into exon 3

548   of the *APP* gene, and then with gancyclovir to select for loss of the chromosome

549   21 bearing the inserted selection cassette. It is possible that these rounds of

550   selection resulted in epigenetic (or, less likely, genetic) changes that added to the

551   transcriptional differences between the trisomic and disomic iPSCs. In fact, we

552   were unable to efficiently differentiate into cortical neuronal cultures any of the 4

553   disomic clones that had gone through these selection procedures. As the

554   differentiation protocol we used has been employed by other research groups to

555   produce cortical neuron cultures from iPSCs with normal karyotypes, we suspect

556   that the derivation of disomic clones may have resulted in a subtle intrinsic

557   change in the iPSC state. Fortunately, we were able to derive a spontaneous

558   disomic line from the C3 trisomic iPSC clone, which did readily differentiate into

559   cortical neurons. The C3 disomic iPSCs (C3-D21) were therefore used to

560   generate the disomic cortical neuronal cultures. Importantly, C3-D21 disomic

561   iPSCs expressed less MAP2 than trisomic iPSCs (Figure 3C), and we still

562   observed increased expression of neuronal-associated genes in the C2 trisomic

563   neuronal cultures compared to the disomic neuronal cultures derived from C3-

564   D21. These observations argue that our finding that C2 trisomic cells have a

565   more neuronal character than disomic cells from the same individual cannot be

566   attributed to an artifact of the genetically-selected disomic clones.

567

568   The neuronal differentiation protocol we used (Espuny-Camacho et al, 2013)

569   has been reported to result in the production of layer V and VI cortical neurons

570   after 40 days in culture, which we confirmed by immunofluorescence microscopy

571   using antibodies against layer V and VI - specific transcription factors CTIP2 and

572   TBR1, as well as antibodies to glutamate receptor GRIK2 and glutamate

573   transporter vGLUT1 (Supplementary Figure 1). While the neuronal cultures

574   derived from the trisomic and disomic iPSCs were not readily distinguishable

575   using any of these markers, there were significant transcriptome differences. Of

576   particular note was increased transcript accumulation for synaptic proteins,

577   including GABA (GABRG2, GABRA1, GABRB2, GABBR2) and glutamate

578   (GRIN2B, GRIA1) receptors in the trisomic iPSC-derived neuronal cultures.   We

579   note that increased GABAnergic signaling occurs in the Ts65Dn mouse DS

580   model (Kleschevnikov et al, 2012a), and counteracting GABAnergic inhibition in

581   these mice reverses behavioral deficits (Kleschevnikov et al, 2012b).

582

583   *Transcriptome characteristics not affected by chromosome 21 trisomy.*

584

585   The increased chromosome 21 gene dosage in trisomic cells could conceivably

586   affect global RNA metabolism, as chromosome 21 encodes the RNA editing

587   gene ADARB1 and multiple splicing factors (including U2AF1, SON and SCAF4).

588   Global chromatin effects of chromosome 21 trisomy were also proposed by

589   Letourneau et al (2014), who identified gene expression dysregulation domains

590   (GEDDs) in trisomic iPSCs and fibroblasts. We have analyzed our transcriptome

591   data for trisomy-dependent changes in adenosine-to-inosine RNA editing,

592   alternative splicing, repetitive element expression, and chromosomal domains of

593   altered expression. Examining more than 10,000 annotated RNA editing sites

594   (from the DARNED database), we did not find any evidence for global changes in

595   RNA editing in trisomic iPSC-derived neuronal cultures. This analysis does not

596   preclude changes in site-specific editing, which would require significantly deeper

597   sequencing depth to assay accurately. Nevertheless, our data indicate that

598   global editing levels do not correlate with ADARB1 transcript levels, likely due to

599   the multiple factors that control the accumulation of edited transcripts. Our data

600   also did not reproduce the gene expression domains identified by Letourneau et

601   al (2014), and we note that an independent analysis of the Letourneau data has

602   questioned the existence of GEDDs (Do et al., 2015).

603

604   *Altered splicing in trisomic cells.*

605

606   We did observe trisomy-dependent splicing changes in both the iPSCs and

607   neuronal cultures. Our identification of splicing alterations in trisomic cells is not

608   completely novel, as splicing differences in a selected set of genes has been

609   observed in fetal DS tissue (Toiber et al, 2010). RNA-seq has also been used

610   previously to support altered splicing in DS endothelial progenitor cells, although

611   no confirmatory studies were done (Costa et al, 2011). The large majority of

612   splicing changes we identified did not occur in genes located on chromosome 21,

29

613   suggesting that they were not a direct effect of gene dosage (i.e., higher gene

614   dosage leading to competition for splicing factors and subsequent altered

615   splicing). More likely is the possibility that altered expression or altered activity of

616   splicing factors caused the splicing dysregulation observed in trisomic cells. We

617   did observe increased transcript accumulation for three known or suspected

618   splicing factors (U2AF1, SON, and SCAF4) located on chromosome 21 in the

619   trisomic iPSC and/or neuronal cultures. Alternatively, increased expression of

620   chromosome 21 gene DYRK1A, a kinase known to regulate splicing factors

621   (Qian 2011), could contribute to the splicing changes we identified. Over-

622   expression of DYRK1A in mice has been reported to mimic Down syndrome

623   splicing aberrations (Tobier et al, 2010). Direct demonstration of a role of

624   DYRK1A or specific splicing factors in the trisomy-dependent splicing changes

625   we have observed will require additional studies in which the gene dosage or

626   expression levels of these genes are normalized in trisomic backgrounds.

627

628   *Altered HERVH expression in trisomic iPSCs.*

629

630   Examination of the accumulation of repetitive element transcripts revealed a

631   highly significant decrease in transcripts from the endogenous retrovirus HERVH

632   in the trisomic iPSCs. HERVH transcripts have been specifically identified as a

633   pluripotency marker (Santoni et al, 2012), and disruption of HERVH transcription

634   compromises self-renewal in human embryonic stem cells (Wang et al, 2014).

635   The reduced HERVH expression we observe in trisomic iPSCs is consistent with

636   these cells having an altered pluripotent state in comparison to the disomic

637   iPSCs.

638

639   *Comparison with other datasets.*

640

641   As described above, consideration of the possible effects of the selection

642   procedures used to generate the disomic derivative clones suggests a possible

643   technical reason why we have observed transcriptional differences not reported

644   by other investigators. However, cluster analysis of our dataset with other

645   comparable studies suggests that our results are not anomalous, but may reflect

646   the range of states assumed by human stem cells trisomic for chromosome 21.

647   The dendrogram shown in figure 6A could be interpreted as showing that there

648   are two classes of trisomic stem cells: one class with a more neuronal character

649   (cells from this study, the twin study of Letourneau et al, and clone 3 from the

650   Jiang study), and one class with a more mesodermal character (clones 1 and 2

651   from the Jiang study, and both trisomic lines from the Wieck et al study). This is

652   likely an oversimplification; more extensive data might readily reveal a spectrum

653   of trisomic stem cell fates. However, this analysis does suggest that there is

654   unlikely to be a single transcriptome signature for trisomic stem cells, and the

655   observed transcriptome variation may not simply be a result of varying

656   experimental conditions. This latter point is supported by the observation that

657   clone 3 of the Jiang et al study clustered more closely with our data set than with

658   the other XIST clones. The Jiang study was particularly well controlled, as the

659   iPSCs were grown under the same conditions (using mouse embryonic

660   fibroblasts as feeder cells) with the same length of XIST-based knockdown of

661   chromosome 21 expression (3 weeks). Nevertheless, clone 3 trisomic iPSCs

662   appeared more similar to ours, which were grown in feeder-free media.

663

664   *Chromosome 21 trisomy and stem cell pluripotency.*

665

666   Why might trisomic iPSCs show a range of transcriptome signatures? Given

667   our observation that the trisomic iPSCs we characterized had enhanced

668   accumulation of transcripts associated with differentiated neurons, and reduced

669   expression of the HERVH pluripotency marker, we speculate that trisomic iPSCs

670   may have an inherent inability to maintain a full pluripotent state. Following this

671   assumption, trisomic iPSCs would have a more constrained differentiation

672   capacity than corresponding disomic iPSCs, which could explain their reported

673   defects in neuronal differentiation (Jiang et al, 2013). On the other hand, in the

674   absence of full pluripotency, trisomic iPSCs might alternatively be biased towards

675   ectodermal fates (e.g., the trisomic iPSCs we have characterized). The specific

676   developmental bias of a given trisomic iPSC might depend on a variety of factors:

677   genetic background, initial culture conditions, pluripotency factor expression, or

678   stochastic variation. If the gene dosage burden imposed by chromosome 21

679   trisomy generally interferes with the maintenance of stem cell fate, this might

680   account for some Down syndrome clinical phenotypes, including the

681   hematopoietic developmental defects observed in DS (Roberts and Izraeli,

682   2014). In this regard, it has been reported that the Ts65Dn mice have defects in

683   the self-renewal of hematopoietic stem cells as well as in the expansion of

684   mammary epithelial cells, neural progenitors and fibroblasts, specifically due to

685   the triplication of Usp16 (Adorno et al, 2013).

686

Gonzales et al.   "Transcriptome analysis in trisomy 21"

33

Literature cited

687

688

689   1.   M. Adorno *et al.*, Usp16 contributes to somatic stem-cell defects in Down's

690   syndrome. *Nature* **501**, 380-384 (2013).

691   2.   S. Anders, W. Huber, Differential expression analysis for sequence count

692   data. *Genome Biol* **11**, R106 (2010).

693   3.   Andrews S. FastQC: a quality control tool for high throughput sequence

694   data. (2010). Available online at:

695   http://www.bioinformatics.babraham.ac.uk/projects/fastqc

696   4.   A. M. Bolger, M. Lohse, B. Usadel, Trimmomatic: a flexible trimmer for

697   Illumina sequence data. *Bioinformatics* **30**, 2114-2120 (2014).

698   5.   V. Costa *et al.*, Massive-scale RNA-Seq analysis of non ribosomal

699   transcriptome in human trisomy 21. *PLoS One* **6**, e18493 (2011).

700   6.   S. W. Criscione, Y. Zhang, W. Thompson, J. M. Sedivy, N. Neretti,

701   Transcriptional landscape of repetitive elements in normal and cancer

702   human cells. *BMC Genomics* **15**, 583 (2014).

703   7.   M. J. de Hoon, S. Imoto, J. Nolan, S. Miyano, Open source clustering

704   software. *Bioinformatics* **20**, 1453-1454 (2004).

705   8.   I. Espuny-Camacho *et al.*, Pyramidal neurons derived from human

706   pluripotent stem cells integrate efficiently into mouse brain circuits in vivo.

707   *Neuron* **77**, 440-456 (2013).

708   9.   A. Fort *et al.*, Deep transcriptome profiling of mammalian stem cells

709   supports a regulatory role for retrotransposons in pluripotency

710   maintenance. *Nat Genet* **46**, 558-566 (2014).

711   10.   K. Gardiner *et al.*, Down syndrome: from understanding the neurobiology

712   to therapy. *J Neurosci* **30**, 14943-14945 (2010).

713   11.   N. Gaspard, A. Gaillard, P. Vanderhaeghen, Making cortex in a dish: in

714   vitro corticopoiesis from embryonic stem cells. *Cell Cycle* **8**, 2491-2496

715   (2009).

716   12.   F. Guedj *et al.*, The fetal brain transcriptome and neonatal behavioral

717   phenotype in the Ts1Cje mouse model of Down syndrome. *Am J Med*

718   *Genet A* **167A**, 1993-2008 (2015).

719   13.   S. W. Hartley, J. C. Mullikin, QoRTs: a comprehensive toolset for quality

720   control and data processing of RNA-Seq experiments. *BMC Bioinformatics*

721   **16**, 224 (2015).

722   14.   S. W. Hartley, J. C. Mullikin, Detection and visualization of differential

723   splicing in RNA-Seq data with JunctionSeq. *Nucleic Acids Res* **44**, e127

724   (2016).

725   15.   J. Jiang *et al.*, Translating dosage compensation to trisomy 21. *Nature*

726   **500**, 296-300 (2013).

727   16.   D. Kim *et al.*, TopHat2: accurate alignment of transcriptomes in the

728   presence of insertions, deletions and gene fusions. *Genome Biol* **14**, R36

729   (2013).

730   17.   A. Kiran, P. V. Baranov, DARNED: a DAtabase of RNa EDiting in humans.

731   *Bioinformatics* **26**, 1772-1776 (2010).

732   18.   A. M. Kleschevnikov *et al.*, Deficits in cognition and synaptic plasticity in a

733   mouse model of Down syndrome ameliorated by GABAB receptor

734   antagonists. *J Neurosci* **32**, 9217-9227 (2012).

735   19.   A. M. Kleschevnikov *et al.*, Increased efficiency of the GABAA and

736   GABAB receptor-mediated neurotransmission in the Ts65Dn mouse

737   model of Down syndrome. *Neurobiol Dis* **45**, 683-691 (2012).

738   20.   A. Letourneau *et al.*, Domains of genome-wide gene expression

739   dysregulation in Down's syndrome. *Nature* **508**, 345-350 (2014).

740   21.   H. Li *et al.*, The Sequence Alignment/Map format and SAMtools.

741   *Bioinformatics* **25**, 2078-2079 (2009).

742   22.   L. B. Li *et al.*, Trisomy correction in Down syndrome induced pluripotent

743   stem cells. *Cell Stem Cell* **11**, 615-619 (2012).

744   23.   Y. Liao, G. K. Smyth, W. Shi, The Subread aligner: fast, accurate and

745   scalable read mapping by seed-and-vote. *Nucleic Acids Res* **41**, e108

746   (2013).

747   24.   K. H. Ling *et al.*, Functional transcriptome analysis of the postnatal brain of

748   the Ts1Cje mouse model for Down syndrome reveals global disruption of

749   interferon-related molecular networks. *BMC Genomics* **15**, 624 (2014).

750   25.   B. Liu, S. Filippi, A. Roy, I. Roberts, Stem and progenitor cell dysfunction

751   in human trisomies. *EMBO Rep* **16**, 44-62 (2015).

752   26.   C. Liu *et al.*, Mouse models for Down syndrome-associated developmental

753   cognitive disabilities. *Dev Neurosci* **33**, 404-413 (2011).

754   27.   T. S. Macfarlan *et al.*, Embryonic stem cell potency fluctuates with

755   endogenous retrovirus activity. *Nature* **487**, 57-63 (2012).

756   28.   J. L. Olmos-Serrano *et al.*, Down Syndrome Developmental Brain

757   Transcriptome Reveals Defective Oligodendrocyte Differentiation and

758   Myelination. *Neuron* **89**, 1208-1222 (2016).

759   29.   M. C. Potier *et al.*, Transcriptional disruptions in Down syndrome: a case

760   study in the Ts1Cje mouse cerebellum during post-natal development. *J

761   Neurochem* **97 Suppl 1**, 104-109 (2006).

762   30.   W. Qian *et al.*, Regulation of the alternative splicing of tau exon 10 by

763   SC35 and Dyrk1A. *Nucleic Acids Res* **39**, 6161-6171 (2011).

764   31.   I. Roberts, S. Izraeli, Haematopoietic development and leukaemia in Down

765   syndrome. *Br J Haematol* **167**, 587-599 (2014).

766   32.   A. J. Saldanha, Java Treeview--extensible visualization of microarray data.

767   *Bioinformatics* **20**, 3246-3248 (2004).

768   33.   F. A. Santoni, J. Guerra, J. Luban, HERV-H RNA is abundant in human

769   embryonic stem cells and a precise marker for pluripotency. *Retrovirology*

770   **9**, 111 (2012).

771   34.   N. G. Saran, M. T. Pletcher, J. E. Natale, Y. Cheng, R. H. Reeves, Global

772   disruption of the cerebellar transcriptome in a Down syndrome mouse

773   model. *Hum Mol Genet* **12**, 2013-2019 (2003).

774   35.   Y. Shi, P. Kirwan, J. Smith, H. P. Robinson, F. J. Livesey, Human cerebral

775   cortex development from pluripotent stem cells to functional excitatory

776   synapses. *Nat Neurosci* **15**, 477-486, S471 (2012).

777   36.   K. D. Sullivan *et al.*, Trisomy 21 consistently activates the interferon

778   response. *Elife* **5**, (2016).

779   37.   D. Toiber *et al.,* Engineering DYRK1A overdosage yields Down syndrome-

780   characteristic cortical splicing aberrations. *Neurobiol Dis* **40**, 348-359

781   (2010).

782   38.   J. Wang *et al.,* Primate-specific endogenous retrovirus-driven transcription

783   defines naive-like stem cells. *Nature* **516**, 405-409 (2014).

784   39.   J. P. Weick *et al.,* Deficits in human trisomy 21 iPSCs and neurons. *Proc*

785   *Natl Acad Sci U S A* **110**, 9962-9967 (2013).

786

Gonzales et al.   "Transcriptome analysis in trisomy 21"

38

787   **Supplemental Figures**
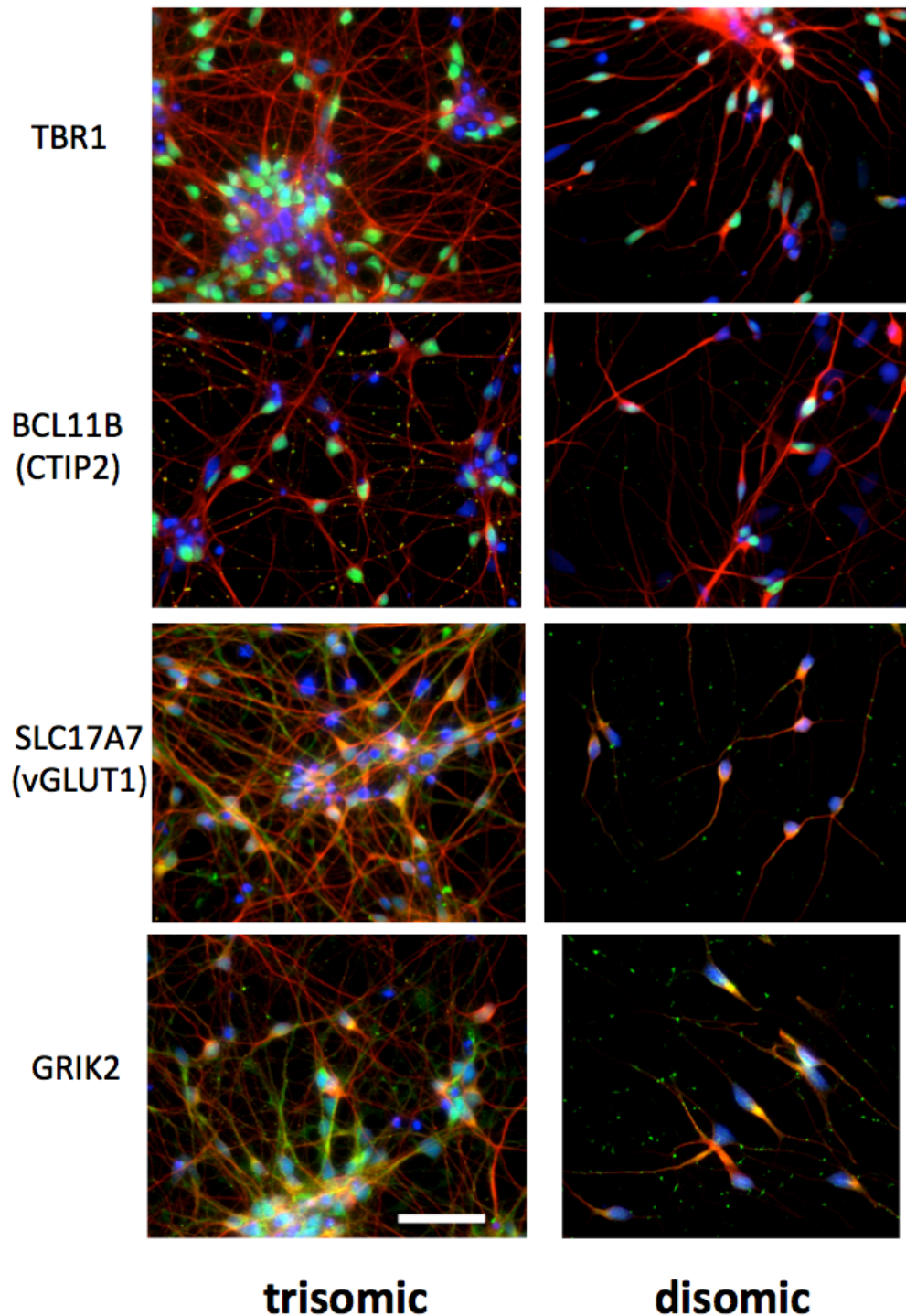
trisomic   **disomic**

788

789   **Supplemental Figure 1.** Confirmation of differentiation of iPSCs into cortical

790   neuronal cultures. Images taken from clones C2 (trisomic) and C3 -D21

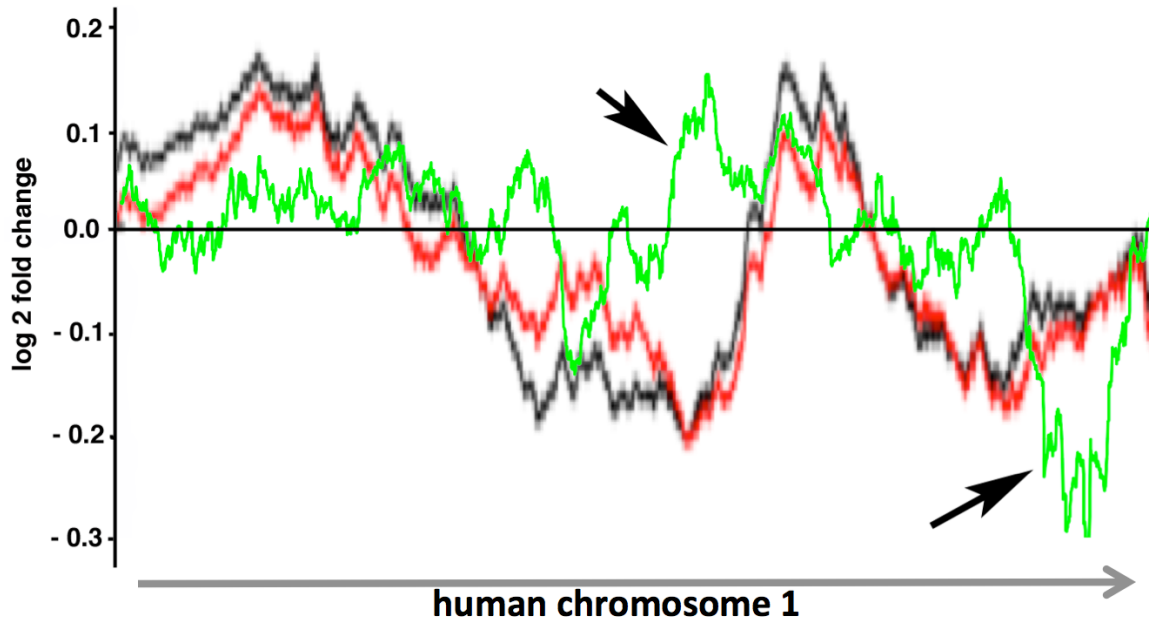791   (disomic) 40 days after initiation of the differentiation protocol. Fixed cells on

792   chamber slides were probed with antibodies against the marker proteins listed in

793   the left column. Neuronal marker Beta III tubulin is red; DAPI is blue; and Ctip2,

794   TBR1, SLC17A7 (vGLUT1) and GRIK2 are green.   Size bar = 20 microns.

795

796

797

798

799   **Supplementary Figure 2.** Comparison of putative trisomy-dependent gene

800   expression domains identified on chromosome 1 by Letourneau et al (2014) and

801   this study. Lines show regions of increased or decreased gene expression in

802   cells trisomic for chromosome 21 as calculated using the smoothing algorithm

803   employed by Letourneau et al. The red (iPSCs) and black (fibroblast) traces are

804   taken from the Letourneau study; the green trace is from the iPSCs used in this

805   study. Note that there are significantly different expression domains calculated

806   from the different studies (arrows).

807

808

809